厚生科学研究費補助金（がん臨床研究事業）

II-15 分担研究報告書

研究分担者　栃木　達夫

早期前立腺癌に対する各種根治療法の臨床病理的検討

研究要旨
早期前立腺癌に対する各種根治療法の成績に関する臨床的および病理組織学的検討を行った。

研究分担者氏名：　栃木達夫
所属機関名、職名：宮城県立がんセンター
医療部長

A. 研究目的

前立腺癌に対する内分泌・放射線併用療法の治療成績を後ろ向きに検討した。

B. 研究方法

対象は''97年2月から'08年7月の間に内分泌・放射線併用療法を行った前立腺癌 275 例（cT1c:9 例、cT2 :134 例、cT3 :132 例）。年齢は 55 歳～85 歳（平均 72.2 歳）、癌発見時 PSA 値は 1.9～710ng/ml（中央値 12.0 ng/ml）、生検 Gleason score(生検 GS) は 6 以下:115 例、7：89 例、8 以上：71 例。治療方法:まず内分泌療法を先行させてから外照射を行うか、内分泌療法開始とほぼ同時に施行した。照射線量は 70～72Gy である。観察期間は 192 日～4526 日（中央値 1402 日）。

C. 研究結果

観察期間中、癌死を 5 例、他因死を 23 例認めた。275 例の 5 年、10 年全生存率は、各々88.1%、76.2%で、5 年、10 年癌特異生存率は、98.1%,90.5%であった。診断時 PSA 値を≦10、10.1～20、20.1～40、40<と分けた場合の 5 年全生存率は、90.6%,92.1%、86.4%、78.2%で、診断時 PSA 値が≦10 と 40<の間に有意差を認めた(<0.05)。生検 GS 別の 10 年全生存率は、6 以下:89.3%、7：80.6%、8 以上：46.9%で、生検 GS6 以下と 8 以上の間に有意差を認めた(<0.05)。臨床病期別では cT2 と cT3 の 10 年全生存率は、84.6%と 69.3%であったが二群間に有意差を認めなかった。診断時 PSA 値、生検 GS、臨床病期と全生存率との関係を多変量解析すると生検 GS 8 以上のみが有意に全生存率と関連していた。晩期有害事象で多いのは、頻尿（6.2%）、尿失禁(4.4%)、放射線直腸炎（4%）、放射線膀胱炎(2.9%)等であった。

D. 考察

前立腺癌に対する放射線治療（外照射）単独よりも内分泌併用放射線治療の成績のほう良好である。IMRT は限られた数少ない施設でのみ可能であるのが現状であり、この状況下では内分泌併用放射線治療による成績向上を目指すのが現実的であろう。しかし、生検 GS 8 以上では内分泌併用の IMRT を目指すべきと思われた。また、晩期有害事象の軽減のためにも IMRT が望ましいと思われた。

E. 結論

1）cT2～T3N0M0 前立腺癌に対する内分泌・放射線併用療法は有用と思われる。
2）生検 GS 8 以上のみが有意に全生存率不良であった。
3）照射法の改善による晩期有害事象の軽減が課題である。

G. 研究発表

1. 論文発表

1. Minami Y, Tochigi T, Kawamura S, et al. Height, urban-born, and prostate cancer risk in Japanese men. Jpn J Clin Oncol 38, 205-213, 2008.
2. Ishidoya S, Ito A, Orikasa K, et al. The outcome of prostate cancer screening in a normal Japanese population with PSA of 2-4 ng/ml and the free/total PSA under 12%. Jpn J Clin Oncol 38, 844-848, 2008.

1. 学会発表

1. 栃木達夫[1]、青木大志[1]、川村貞文[1]、立野紘雄[2]（宮城県立がんセンター泌尿器科[1]、同病理[2]）：前立腺癌に対する内分泌・放射線併用療法の治療成績. 第 46 回日本癌治療学会総会. 名古屋. 2008.11 月.

H. 知的財産権の出願・登録状況

1. 特許取得 なし
2. 実用新案登録　なし

厚生科学研究費補助金（がん臨床研究事業）

II-16 分担研究報告書

研究分担者　野口正典

転移性前立腺癌に対する新規治療法の開発に関する研究

研究要旨
転移性前立腺癌におけるテーラーメイド型癌ペプチドワクチン療法の基礎ならびに臨床研究

研究分担者氏名：　野口正典
所属機関名、職名：久留米大学泌尿器科　准教授

A. 研究目的

再燃前立腺癌患者を対象に、HLA-A24 及び A2 癌ペプチドワクチンの第 II 臨床試験を実施して、その安全性、ペプチド特異的誘導能、及び臨床効果を解析する。本研究のテーマは以下の通りである。

1）再燃前立腺癌に対して臨床効果の向上を目的に新規ペプチドでの試験、およびエストラムスチンとの併用効果を重点的に解析する。

2）HLA-A24 及び A2 前立腺癌に対する新規ペプチド開発のために、前立腺における各種抗原を分析し、前立腺癌患者の IgG 抗体により認識される抗原ペプチドを ELISA 法で同定する。

B. 研究方法

①投与ペプチドへの免疫反応性解析：これまで臨床研究で安全性を確認済みのペプチド 22 種類（HLA-A2 患者用 10 種類、HLA-A24 患者用 12 種類）について、これまで投与を受けた前立腺がん患者での投与前後のサンプルを用いて、ペプチド特異的細胞性免疫能（CTL 活性）及びペプチド特異的液性免疫〈免疫グロブリン、Ig〉を解析する。

②候補ペプチドの選択：①の解析結果より、前立腺がん患者の５０%以上においてペプチド特異的な免疫賦活を認めたペプチドを候補ペプチドとして次の③と④研究に供与する。

③候補ペプチドを混合剤とした場合の溶解性・安定性の検討：②にて選択したペプチドを HLA－A2, A24 各々1 種類での混合剤を作成してその溶解性、安定性、乳化度（アジュバントでの）について検討する。

④臨床試験（橋渡し研究）：　ペプチドワクチンの第 II 相臨床試験〈橋渡し研究〉を実施してその安全性と免疫賦活能を解析する。

C. 研究結果

標準治療（エストラムスチン単独）と、テーラメイドペプチドワクチン+低用量エストラムスチン併用療法の無作為比較試験の中間解析結果では、これまでの標準治療に比較して有意に無増悪期間の延長を認めた。

D. 考察

再燃前立腺癌に関しては、第 I 相臨床試験においてペプチドワクチン療法の安全性が確認され，さらに数例においては PSA の低下、骨転移の消失が認められた。また、低用量エストラムスチン併用で臨床効果が増すことや、低容量でのエストラムスチン併用ではペプチドワクチン療法による免疫反応を抑制しないことが判明した。これらの結果を基に標準治療とペプチドワクチン＋低用量エストラムスチン併用療法との無作為比較試験を行ったが、中間解析にて有意に無増悪期間の延長を認めペプチドワクチンの有用性が示された。

E. 結論

進行前立腺がん患者に対して、テーラーメイドがんペプチドワクチン臨床試験を施行してきた。その結果、皮膚反応以外には有害事象が殆ど無く安全性が確認されたこと、免疫反応性が大多数の症例で確認されたこと、及び一部の患者さん、とりわけ再燃前立腺がん患者では、生命予後延長を認めるにいたった.

G．研究発表

1.　論文発表

1. Noguchi M, Kakuma T, Suekane S, et al. A randomized clinical trial of suspension technique for improving early recovery of urinary continence after radical retropubic prostatectomy. BJU Int 102: 958-963, 2008.

1. Noguchi M, Todo S, Yanagimoto H, et al. Immunological and clinical effects of personalized peptide vaccine for HLA-A2 positive patients with advanced cancer. ASCO 2008 (American Society of Clinical Oncology) Annual Meeting

H. 知的財産権の出願・登録状況

1. 特許取得 なし
2. 実用新案登録　なし

厚生科学研究費補助金（がん臨床研究事業）

II-17 分担研究報告書

研究分担者　筧　善行

早期前立腺癌に対する根治術後のQOLの解析と新たなbiomarkerの開発に関する研究

研究要旨
早期前立腺癌に対する外科療法、放射線療法、PSA 監視療法（無治療経過観察）などの患者 QOL に及ぼす影響を解析した。前立腺がんの悪性進展に関与する新規分子マーカーの検討を行った。

研究分担者氏名：　筧　善行
所属機関名、職名：香川大学泌尿器科　教授

A. 研究目的

1）PSA テストの普及で早期前立腺癌が急増しているが、患者の精神的・身体的健康観（QOL）に及ぼす影響に関しては不明な点が多く、QOL に関する客観的情報を蓄積することを目的とした。
2）早期前立腺癌の適切な治療選択のためには、PSA をしのぐ新規分子マーカーの開発が急務である。

B. 研究方法

1）stage T1c, PSA<20ng/ml, Gleason score<7, 陽性生検コア≦ 2 本, 陽性コアにおける最大腫瘍占拠面積≦50%の条件で選択された日本人患者で PSA監視療法を選択した 99 名に関して登録時と 1 年後に SF-36 を用いて QOL を測定した。
2）日本語版 EPIC（限局性前立腺癌特異的 QOL 調査票：米国で開発）の妥当性試験に参加した患者に関して、日本語版 SF-8 を用いて一般的健康関連 QOL を測定し、各治療法別に比較した。
3）限局性前立腺癌に対して前立腺全摘除を行った患者群の術後排尿機能を IPSS を用いて測定し、高齢女性と比較した。
4）生理活性脂質 LPA 関連分子群（合成酵素 2 種、受容体 3 種、代謝酵素 1 種）の mRNA 発現レベルを、LCM 法にて前立腺癌細胞、癌周囲間質細胞、前癌病変、両性腺細胞などに分けて解析した。さらに前立腺全摘標本における LPA 合成酵素 AGK(acylglycerol kinase)と ATX (autotaxin) のタンパク発現を解析し、臨床病理学的パラメーターとの関連を解析した。

C. 研究結果

1）早期癌で PSA監視療法施行 1 年後の一般的QOL は悪化していなかった。
2）外科的治療群では術後 1 年以後の mental および physical summary score の改善傾向が明らかであった。一方、放射線外照射療法患者の治療後の physical summary score の低下が目立った。
3）前立腺全摘後の（男性）患者は畜尿機能に劣る排尿機能パターンを示し、高齢女性の排尿機能パターンに類似していた。
4）LPA 合成酵素の一つである ATX の発現上昇は前立腺全摘後の PSA 再燃を予測する独立した予後因子であった。

D. 考察

限局性前立腺癌に対する治療に伴う患者 QOL への影響は、治療法により障害プロフィルや経時的変化のパターンが異なることが示された。生理活性脂質 LPA は前立腺癌の発生および悪性進展の両者に関連することが示唆された。特に LPA 合成酵素である ATX は予後予測因子として有用である可能性が示唆された。

E. 結論

前立腺癌患者における各種治療法のアウトカム評価において、QOL 評価は重要な評価項目である。LPA 合成酵素の一つである ATX は限局性前立腺癌の根治治療後の予後予測因子になる可能性がある。

G. 研究発表

1. 論文発表

1. Zeng Y, Kakehi Y, Nouh MA, et al. Gene expression profiles of lysophosphatidic acid-related molecules in the prostate: Relevance to prostate cancer and benign hyperplasia. Prostate 69: 283-292, 2009.
2. Sugimoto M, Takegami M, et al. Health-related quality of life in Japanese men with localized prostate cancer: assessment with the SF-8. Int J Urol 2008 15:524-8.

2. 学会発表

1. 筧　善行, 賀本　敏行, 白石　泰三『Insignficant Prostate Cancer の予測』「生検病理と PSA-kinetics による insignficant cancer の予測.」第 96 回日本泌尿器科学会総会

H. 知的財産権の出願・登録状況

1. 特許取得 なし
2. 実用新案登録　なし

厚生科学研究費補助金（がん臨床研究事業）

II-18 分担研究報告書

研究分担者　中川　昌之

前立腺癌の発生と進展に関する疫学、遺伝子解析研究

研究要旨
早期前立腺癌に対する根治術後のQOLの解析と新たなbiomarkerの開発に関する研究

研究分担者氏名：　中川　昌之
所属機関名、職名：鹿児島大学泌尿器科　教授

A. 研究目的

癌化のメカニズムとしては，がん遺伝子の活性化やがん抑制遺伝子の不活化に加えて、DNA のメチル化も重要である。近年、前立腺癌では癌抑制遺伝子や細胞間接着分子関連遺伝子のプロモーター領域がメチル化してその発現が抑制されていることが報告されている。我々は前立腺癌における RASSF1A 遺伝子や GSTP1 遺伝子のメチル化検出が新規 biomarker になりうるかを検討した。

B. 研究方法

癌化のメカニズムとしては，がん遺伝子の活性化やがん抑制遺伝子の不活化に加えて、DNA のメチル化も重要である。近年、前立腺癌では癌抑制遺伝子や細胞間接着分子関連遺伝子のプロモーター領域がメチル化してその発現が抑制されていることが報告されている。我々は前立腺癌における RASSF1A 遺伝子や GSTP1 遺伝子のメチル化検出が新規 biomarker になりうるかを検討した。

C. 研究結果

臨床検体における RASSF1A のメチル化異常の頻度は PC　97 例（74.0%），BPH　12 例（18.5%）であった．Gleason スコアが高値な症例や進行した病期のものは有意にメチル化の頻度が高かった．PC におけるメチル化の頻度はこれまでの報告とほぼ同程度であった．前立腺正常細胞においてプロモーター領域は非メチル化の状態であり，mRNA の発現が認められた．一方，前立腺癌細胞ではメチル化しており，mRNA の発現は認めなかった．またヒストン脱アセチル化酵素阻害剤（TSA）単独による発現回復は認めなかったが，DAC との併用による相乗効果を認めた．TSA の併用により発現の増強が得られたことより，RASSF1A の発現抑制の機序としてヒストン修飾の関与が示唆された。前立腺正常細胞ではヒストンのアセチル化を認めたが癌細胞においては認めず，不活性型のヒストン修飾パターンとなっていた．

D. 考察

DAC の投与によりヒストンのアセチル化が認められたが，TSA 単独投与ではヒストン修飾の変化はなかった．以上の結果より前立腺癌における RASSF1A の発現低下には DNA のメチル化とともにヒストン修飾が関与していることが示された．同時に DAC が DNA のメチル化のみならずヒストン修飾も変化させることから，この 2 つの現象の間には DNA methyltransferase を介する相互関係の存在が示唆された。

E. 結論

前立腺癌におけるRASSF1AやGSTP1遺伝子のメチル化検出は新規biomarkerになりうる可能性がある。

G．研究発表

1.　論文発表

1. Kawamoto K, Okino ST, Place RF, et al. Epigenetic modifications of RASSF1A gene through chromatin remodeling in prostate cancer. Clin Cancer Res 13: 2541-2548, 2007.

2.　学会発表

2007 AUA annual meeting, 2007 May (Los Angels). EPIGENETIC MODIFICATIONS OF RASSF1A GENE THROUGH CHROMATIN REMODELING IN PROSTATE CANCER.

H. 知的財産権の出願・登録状況

1. 特許取得 なし
2. 実用新案登録　なし

II-19 分担研究報告書

研究分担者　塚本　泰司

前立腺癌の発生と進展に関する疫学、遺伝子解析研究

研究要旨
前立腺癌の進展に関する臨床的検討を行った。根治的前立腺的除標本の外科切除縁陽性には術前の PSA 値、病理学的病期、生検陽性割合が関与していた。切除縁陽性は PSA 再発のリスク要因であった。

研究分担者氏名：　塚本泰司
所属機関名、職名：札幌医科大学泌尿器科　教授

A. 研究目的
根治的前立腺的除標本の外科切除縁（SM）陽性は PSA 再発のリスク要因であるが、これを予測する術前因子を検討した。さらに、切除縁陽性患者における PSA 再発の予後因子についても検討した。

B. 研究方法
根治的前立腺摘（＋骨盤リンパ節郭清）を行った 238 例の患者を対象とした。PSA 再発は、感度以下に低下した PSA が 0.2ng/ml を超えた場合とした。

C. 研究結果
238 例中、82 例（34.4%）に SM 陽性が認められた。多変量解析では、術前 PSA 値（10ng/ml 以上）、臨床病期（T2a 以上）、陽性生検割合（35%以上）が SM 陽性を予測する因子として同定された。中央値 31.2 か月の経過観察で、48 例（20.2%）に PSA 再発が出現した。5 年 PSA 非再発率は、SM 陰性患者で 81.7%、陽性患者で 62.6%と明らかに差があった。Cox の比例ハザードモデルでは、術前 PSA（20.0ng/ml 以上）、病理学的病期（T3a/T3b）が SM 陽性患者における PSA 再発のリスク因子であった。

D. 考察
SM陽性がPSA再発に強く関与するかどうかに関しては、これまでも異なった結果が出ていたが、今回の検討からは SM の状況は PSA 再発に影響することが明らかとなった。これらのリスク要因が全くないか、あるいは 1 個のみの場合には PSA 再発のリスクは低いが、複数になるとリスクが大きくなることも判明した。

E. 結論
SMの状態は術前のPSA値、臨床病期、生検陽性割合から予測することが可能であった。SM陽性はPSA再発のリスク因子であった。

G. 研究発表
1. 論文発表
1. Hashimoto K, Masumori N, Takei F, et al. Prognostic value of surgical margin status for diease progression following radical prostatectomy. Jpn J Clin Oncol, 38: 31-35, 2008.
2. Hisasue S, Yanase m, Shindo T, et al. Influence of body mass index and total testosterone level on biochemical recurrence following radical prostatectomy. Jpn J Clin Oncol, 38: 129-133, 2008.
3. Furuya R, Hisasue S, Furuya S, et al. The fate of the seminal vesicle following medical castration: how long is the optimal duration of neoadjuvant treatment for prostate cancer before radiation. Urology 72: 417-421, 2008.

2. 学会発表

H. 知的財産権の出願・登録状況
1. 特許取得 なし
2. 実用新案登録

厚生科学研究費補助金（がん臨床研究事業）

II-20 分担研究報告書

研究分担者　宮永　直人

前立腺癌の発生と進展に関する疫学、遺伝子解析研究

研究要旨
大豆イソフラボンによる前立腺癌発癌抑制メカニズムの基礎的検討を行った。

研究分担者氏名：　宮永直人
所属機関名、職名：筑波大学泌尿器科　講師

A. 研究目的

大豆イソフラボンによる前立腺癌予防効果は、latent cancer から significant cancer への移行阻止にあるとされ、そのメカニズムとして dehydrotestosteron(DHT)への阻害などが考えられている。一方、アンドロゲン受容体を介さない前立腺癌細胞への直接作用については未解明である。われわれはアンドロゲン感受性前立腺癌細胞 LNCap において、増殖や形質転換に関与する mitogen activated protein kinase (MAPK)カスケードとイソフラボンの作用について検討した。

B. 研究方法

LNCap 細胞を増殖因子除去済みの培養液とともに 24 時間培養し定着させた。イソフラボンのアンドロゲン受容体を介する抑制作用の評価のために、10uM の Bicultamide、25, 50, 100 uM の Equol および Genistein で 1 時間処理した後、10nM の 5α-DHT を添加し刺激を行った。72 時間後までの細胞増殖抑制効果を WST-8 アッセイで評価した。また MAPK カスケードに対する直接作用を評価するために、24 時間定着培養した LNCap 細胞を 25, 50, 100 uM の Equol および Genistein で 1 時間処理した後、20ng/ml の TPA を添加した。15 分後にタンパク質を抽出し、ウエスタンブロットにて MEK1/2 および MAPK のリン酸化蛋白の発現を評価した。72 時間後までの細胞増殖抑制効果を WST-8 アッセイで評価した。

C. 研究結果

5α-DHT 刺激により LNCap 細胞は増殖し、Bicultamide ならびに Equol、Genisitein は増殖抑制効果を示した。TPA 刺激した LNCap 細胞においては、MEK1/2 および MAPK のリン酸化が生じ、Equol および Genistein を添加した LNCap 細胞では、これらのリン酸化が濃度依存性に抑制された。また Equol および Genistein は、72 時間後まで濃度依存性に TPA 刺激した LNCap 細胞の増殖抑制作用を示した。

D. 結論

大豆イソフラボンによる癌発癌抑制メカニズムは、5α-DHT のアンドロゲン受容体を介した細胞増殖抑制作用とは別に、前立腺癌細胞の MAPK カスケードを直接抑制する作用の存在が示唆された。

E. 研究発表

1.　論文発表

1. Fujimoto K, Tanaka M, Hirao Y, et al. Age-stratified serum levels of isoflavones and proportion of equol producers in Japanese and Korean healthy men. Prostate Cancer Prostatic Dis 11:252-257, 2008.

2.　学会発表

H. 知的財産権の出願・登録状況

1. 特許取得　なし
2. 実用新案登録　なし

厚生科学研究費補助金（がん臨床研究事業）

II-21 分担研究報告書

研究分担者　市川　智彦

前立腺癌の発生と進展に関する疫学、遺伝子・蛋白解析研究

研究要旨
前立腺癌の発生や進展に関連する染色体異常について、手術標本においてCGH解析を行うことにより基礎的検討を行った。

研究分担者氏名：　市川智彦
所属機関名、職名：千葉大学泌尿器科　教授

A. 研究目的

前立腺癌は多病巣性に発生することが多いが、それぞれに認められる染色体異常や遺伝子異常の独立性あるいは共通性についてはまだ十分に解明されていない。前立腺癌手術標本に2箇所以上癌病巣が存在するものについて、それぞれDNAを抽出し、染色体の欠失や増幅に共通性が見られるか否かを検討した。

B. 研究方法

前立腺癌に対する前立腺全摘除術で得られた前立腺標本において、癌病巣が2箇所以上確認できた22症例を対象とした。各手術検体においてそれぞれ2箇所の癌病巣（1症例では3箇所）からレーザーキャプチャーマイクロダイセクション法を用いて均一な癌組織を採取し、DNAを抽出した。抽出したDNAを増幅した後、CGH法（comparative genomic hybridization法）を用いて、欠失あるいは増幅している染色体の領域を解析した。

C. 研究結果

22例45箇所の癌病巣において頻度の高い染色体の欠失領域は、2q21-24（22.2%）、6q14-22（60.0%）、8p12-22（35.6%）、13q14-31（44.4%）、16q13-24（24.4%）であった。また、頻度の高い増幅領域は　8q21.3-24.3（37.8%）と　7q21-33（20.0%）であった。8p12-22と16q13-24の欠失ならびに8q21.3-24.3の増幅はGleason score（GS）が低いものより高いものにおいてより頻度が高かった（それぞれ $P<0.01$、$P<0.05$、$P<0.01$）。8p12-22や13q14-31の欠失がみられる癌病巣の方がそうでないものより腫瘍の大きさが大きかった（それぞれ $P<0.05$、$P<0.01$）。同一標本中の2箇所の癌病巣における染色体の欠失と増幅が同じパターンを示したものは1例のみであり、その他の症例ではそれぞれ全く異なった異常を有していた。high GSや被膜外浸潤のみられるような悪性度の高い癌病巣では8p12-22の欠失の頻度が有意に高かった（$P<0.05$）。

D. 考察

前立腺癌において8p12-22の欠失頻度が高いという結果は、我々が従来から行っている一連の研究結果や他施設の結果と一致している。今回、同一標本における複数箇所の癌病巣を解析することにより、癌の発生や進展はそれぞれ独立していることが示されたと考えられる。これは、前立腺癌の多中心性発生を支持する結果である。今回異常を検出できなかった癌病巣においても、array CGHを行うことにより欠失や増幅を検出できる可能性がある。したがって、今後さらにarray CGHを行い、微小欠失や増幅の有無を解析し、多中心性発生の機序をさらに検討していく予定である。

E. 結論

同一前立腺に発生する複数箇所の癌はそれぞれ遺伝的に独立して発生していると考えられる。また、8p12-22の欠失は前立腺癌の進展に深く関連していた。

F. 研究発表

1. 論文発表

1. Kobayashi M, Ishida H, Shindo T, et al. Molecular analysis of multifocal prostate cancer by comparative genomic hybridization. Prostate 68:1715-1724, 2008.

G. 知的財産権の出願・登録状況

1. 特許取得　なし
2. 実用新案登録　なし

厚生科学研究費補助金（がん臨床研究事業）

II-22 分担研究報告書

研究分担者　野村照久

早期前立腺癌に対するミニマム創根治術後の排尿機能に関する検討

研究要旨

早期前立腺癌に対するミニマム創根治的前立腺摘除術後の排尿機能を中心としたQOLを、アプローチ別に検討した。

研究分担者氏名：　野村照久

所属機関名、職名：山梨大学泌尿器科　講師

A. 研究目的

早期前立腺癌に対するミニマム創内視鏡下前立腺全摘除術後の尿失禁の程度を中心に、術後のQOL、手術成績を逆行性アプローチと両行性アプローチの別に比較検討した。

B. 研究方法

早期前立腺癌症37例に対し5-6 cmの下腹部正中切開で逆行性アプローチ（10例）または両行性プローチ（27例）のいずれかでミニマム創内視鏡下前立腺摘除術を施行した（背景に有意差なし）。

C. 研究結果

手術時間:391分 v.s. 327分(逆行性v.s.両行性、以下平均、同順)、出血量(尿含む):1297ml v.s. 1124ml、摘出重量:34.5g v.s. 36.3g、術中合併症なし。術後歩行、食事開始：術後1日目、鎮痛剤使用:2-3日,尿道カテーテル抜去: 8.4日v.s. 5.9日、尿失禁： カテーテル抜去後3日以内に0-1 pad;70% v.s. 70.4%、1ヶ月までに0-1 pad; 30% v.s. 11%,3ヶ月までに0-1 pad; 0% v.s. 19%。病理: cap(+)のみ; 20% v.s. 11%、cap(+)& ew(+); 20% v.s. 14.8%、cap(-)& ew(+); なし。Nadir HS-PSA not detected : 50% v.s. 74%

D. 考察、結論

手術時間、出血量は両行性アプローチの導入により有意に短縮された。また、術後高感度PSAの経過からは、より手技的に容易な両行性アプローチでより根治的な手術が期待できる可能性が考えられた。尿失禁を主体とする術後の排尿状態は両群間で差が無かったが、通常の開腹術と比べれば明らかに有利であった。

G. 研究発表

1. 論文発表

1. Araki I, Tsuchida T, Nomura T, et al. Differential impact of lower urinary tract symptoms on generic and disease-specific quality of life in men and women. Urol Int 81:60-65, 2008.

2. 学会発表

1 Yamagishi T, Zakohji H, Fukazawa M, et al. High Incidence of Non-detected Tumor (pT0) After Neoadjuvant Endocrine Treatment and Radical Prostatectomy Was Not Correlated With Lower Incidence of PSA Recurrence in Localized Pristatic Carcinoma in Yamanashi, Japan. The annual meeting of AUA, (Orland, Florida), 2008.

2. Teruhisa Nomura, Makoto Kawaguchi, et al. Modified retropubic open prostatectomy using a vessel sealing system. Male Voiding Dysfunction, BPH and Didactic Urological Videos Session 1. The annual meeting of AUA, (Orland, Florida), 2008.

3. Akihiro Maniwa, Manabu Kamiyama, Yuuki Mikami, et al. Efficacy and safety of paclitaxel and gemcitabine combination as the chemotherapy for advanced/ metastatic urothelial cancer in a single center in japan. The annual meeting of AUA, (Orland, Florida), 2008.

H. 知的財産権の出願・登録状況

1. 特許取得 なし
2. 実用新案登録　なし

III 研究成果の刊行に関する一覧表

発表者氏名	論文タイトル名	発表誌名	巻号	ページ	出版年
Yoshimitsu K, Kiyoshima K, Irie H, et al.	Usefulness of apparent diffusion coefficient map in diagnosing prostate carcinoma: correlation with stepwise histopathology.	J Magn Reson Imaging	27	132-139	2008
Shimizu Y, Segawa T, Inoue T, et al.	Increased Akt and phosphorylated Akt expression are associated with malignant biological features of prostate cancer in Japanese men.	BJU Int	100	685-690	2007
Ma Z, Tsuchiya N, Yuasa T, et al et al.	Polymorphisms of fibroblast growth factor receptor 4 have association with the development of prostate cancer and benign prostatic hyperplasia and the progression of prostate cancer in a Japanese population.	Int J Cancer	123	2574-2579	2008
Narita N, Tsuchiya N, Saito M, et al.	Candidate genes involved in enhanced growth of human prostate cancer under high fat feeding identified by microarray analysis.	Prostate	68	321-335	2008
Nishimoto K, Nakashima J, Hashiguchi A et al.	Prediction of extraprostatic extension by prostate specific antigen velocity, endorectal MRI, and biopsy Gleason score in clinically localized prostate cancer.	Int J Urol	15	520-523	2008
Satoh T, Ishiyama H, Matsumoto K, et al.	Prostate-specific antigen 'bounce' after permanent (125)I-implant brachytherapy in Japanese men: a multi-institutional pooled analysis.	BJU Int	25	1-5	2008
Miyajima N, Maruyama S, Bohgaki M, et al.	TRIM68 regulates ligand-dependent transcription of androgen receptor in prostate cancer cells.	Cancer Res	68	3486-3494	2008
Takenaka A, Soga H, Kurahashi T, et al.	Early recovery of urinary continence after laparoscopic versus retropubic radical prostatectomy: evaluation of preoperative erectile function and nerve-sparing procedure as predictors.	Int Urol Nephrol		in press	2008

Saito S, Murayama Y, Pan Y, et al.	Haptglobin-β chain defined by monoclonal antibody RM2 as a novel Serum marker for prostate cancer.	Int J Cancer	123	633-640	2008
Usami M, Akaza H, Arai Y et.al.	Bicalutamide 80mg combined with a luteinizing hormone-releasing hormone agonist (LHRH-A) versus LHRH-A monotherapy in advanced prostate cancer : findings from a phase III randomized, double-blind, multicenter trial in Japanese patients.	Prostate Cancer and Prostatic Diseases	10	1-8	2007
Ishidoya S, Ito A, Orikasa K, et al.	The outcome of prostate cancer screening in a normal Japanese population with PSA of 2-4 ng/ml and the free/total PSA under 12%.	Jpn J Clin Oncol	38	844-848	2008
Noguchi M, Kakuma T, Suekane S, et al.	A randomized clinical trial of suspension technique for improving early recovery of urinary continence after radical retropubic prostatectomy.	BJU Int	102	958-963	2008
Zeng Y, Kakehi Y, Nouh MA, et al.	Gene expression profiles of lysophosphatidic acid-related molecules in the prostate: Relevance to prostate cancer and benign hyperplasia.	Prostate	69	283-292	2008
Kawamoto K, Okino ST, Place RF, et al.	Epigenetic modifications of RASSF1A gene through chromatin remodeling in prostate cancer.	Clin Cancer Res	13	2541-2548	2007
Furuya R, Hisasue S, Furuya S, et al.	The fate of the seminal vesicle following medical castration: how long is the optimal duration of neoadjuvant treatment for prostate cancer before radiation.	Urology	72	417-421	2008
Fujimoto K, Tanaka M, Hirao Y, et al.	Age-stratified serum levels of isoflavones and proportion of equol producers in Japanese and Korean healthy men.	Prostate Cancer Prostatic Dis	11	252-257	2008
Kobayashi M, Ishida H, Shindo T, et al.	Molecular analysis of multifocal prostate cancer by comparative genomic hybridization.	Prostate	68	1715-1724	2008

Araki I, Tsuchida T, Nomura T, et al.	Differential impact of lower urinary tract symptoms on generic and disease-specific quality of life in men and women.	Urol Int	81	60-65	2008

Original Research

Usefulness of Apparent Diffusion Coefficient Map in Diagnosing Prostate Carcinoma: Correlation with Stepwise Histopathology

Kengo Yoshimitsu, MD,[1]* Keijiro Kiyoshima, MD,[2] Hiroyuki Irie, MD,[1] Tsuyoshi Tajima, MD,[1] Yoshiki Asayama, MD,[1] Masakazu Hirakawa, MD,[1] Kousei Ishigami, MD,[1] Seiji Naito, MD,[3] and Hiroshi Honda, MD[1]

Purpose: To elucidate the performance of apparent diffusion coefficient (ADC) map in localizing prostate carcinoma (PC) using stepwise histopathology as a reference.

Materials and Methods: Preoperative MR images of 37 patients with PC who had undergone radical prostatectomy were retrospectively evaluated. First, T2-weighted images (T2WI) alone were interpreted (T2WI reading), and then T2WI along with ADC map were interpreted (T2WI/ADC map reading). Sextant-based sensitivity and specificity, and the ratio of the detected volume to the whole tumor volume (% tumor volume) were compared between the two interpretations, and results were also correlated to Gleason's scores (GS). ADC values were correlated to histological grades.

Results: Sensitivity was significantly higher in T2WI/ADC map reading than in T2WI reading (71% vs. 51%), but specificity was similar (61% vs. 60%). By adding ADC map to T2WI, % tumor volume detected increased significantly in transitional zone (TZ) lesions, but not in peripheral zone (PZ) lesions. % tumor volume detected with T2WI/ADC map reading showed a positive correlation with GS of the specimens. Less differentiated PC were associated with lower ADC values and higher detectability.

Conclusion: T2WI/ADC map reading was better than T2WI reading in PC detection and localization. This approach may be particularly useful for detecting TZ lesions and biologically aggressive lesions.

Key Words: prostate carcinoma; MR; diffusion-weighted image; ADC map; localization
J. Magn. Reson. Imaging 2008;27:132–139.

PROSTATE CARCINOMA (PC) is one of the most common malignancies in males, and it accounts for approximately 30,000 new annual deaths in the United States (1). To date, surgical resection of the whole organ has been the only method of eradicating this type of malignancy; however, less invasive alternative local therapies, including intensive modulated radiation therapy (IMRT), high-intensity focused ultrasound (HIFU), and brachytherapy, are being introduced due to the increasing clinical demand for the preservation of functional aspects of the prostate and related organs (2–4).

The current role of MRI in the diagnosis of PC is primarily based on T2-weighted images (T2WI), and this approach has remained relatively limited in terms of usefulness, as it can mainly be used to determine whether or not a lesion extends beyond the confinement of the organ capsule (5), a measure used for determining the indication for radical prostatectomy. Also, in the cases of the less invasive local therapies mentioned above, the current approach is to cover the whole organ, regardless of the location or bulk of the tumor within the organ, provided extracapsular extension of the tumor has been excluded (2–4). Because PC can be multifocal and involve any part of the organ, more precise localization and focal targeting of lesions may be beneficial for patients, potentially rendering retreatment for the recurrent tumors possible, in addition to maximizing the options for the preservation of function.

Various MR approaches have been investigated and applied to localize PC; such attempts have included dynamic studies and MR spectroscopy, which provided promising but inconsistent results (6–16). Diffusion-weighted images (DWI) and calculated apparent diffusion coefficient (ADC) mapping are additional approaches, involving the representation of the Brownian movement of water molecules. This new parameter dif-

[1]Department of Clinical Radiology, Graduate School of Clinical Sciences, Kyushu University, Fukuoka, Japan.
[2]Department of Anatomic Pathology, Graduate School of Clinical Sciences, Kyushu University, Fukuoka, Japan.
[3]Department of Urology, Graduate School of Clinical Sciences, Kyushu University, Fukuoka, Japan.
*Address reprint requests to: K.Y., Department of Clinical Radiology, Graduate School of Medical Sciences, Kyushu University, 3-1-1, Maidashi, Higashi-ku, Fukuoka, 812-8582, Japan.
E-mail kengo@med.kyushu-u.ac.jp
Received December 31, 2006; Accepted August 29, 2007.
DOI 10.1002/jmri.21181
Published online in Wiley InterScience (www.interscience.wiley.com).

fers from conventional T1 or T2 relaxivity, dynamic enhancement characteristics, or spectroscopic information. This DWI or the ADC map has been applied for examining various part of the body, in particular to detect or differentiate malignancies (17–20). Regarding PC, several preliminary investigations have been sporadically reported (21–25), with promising results. In this article, we applied the ADC map obtained from DWI to the diagnosis of PC, and evaluated its performance at detecting and localizing PC using stepwise histopathological data as a gold standard. We also correlated the results to the histological grades of the lesions and Gleason's scores (GS) of the specimens, in order to characterize the potential clinical usefulness of this novel technique.

MATERIALS AND METHODS

Patients

Between January 2000 and March 2004, 124 patients underwent radical prostatectomy at our institute. Among these patients, 37 who had undergone preoperative MRI (including DW imaging) were retrospectively selected, and these 37 patients formed the present study population. One of the 37 subjects had received hormonal therapy prior to surgery. The age of the selected patients ranged from 56 to 75 years old (mean = 66 years). The preoperative prostate-specific antigen (PSA) level ranged from 0.7 to 54.8 ng/mL, with a mean of 11.9 (normal range < 4.00 ng/mL). All subjects had undergone transrectal or transperineal biopsy prior to MR imaging and had been pathologically diagnosed with malignant foci in the prostate. The period between biopsy and MR ranged from six to nine weeks (mean = 7.2 weeks), and the period between MR and surgery ranged from zero to eight weeks (mean = 2.5 weeks). The institutional review board at our hospital did not require that written informed consent be obtained for this study due to its retrospective nature. The current study was designed and performed according to the declaration of Helsinki (26).

MR Equipment and Parameters

A total of two 1.5T units (Magnetom Symphony and Vision; Siemens, Erlangen, Germany) were used with a pelvic multichannel phased-array coil (12 channels). After routine T1-weighted spin-echo (TR/TE/number of excitations [NEX] = 500 msec/12 msec/2) axial images had been obtained, T2-weighted fast spin-echo (TR/TE/Turbo factor/NEX = 3000 msec/102 msec/15/3, slice thickness = 5 mm, interslice gap = 30%) axial and coronal images with axial DWI were obtained using the single-shot spin-echo echo-planar imaging (EPI) technique. The matrix and field-of-view of the T1- and T2-weighted images (T1WI and T2WI) were 256 × 512, and 20 cm, respectively. The slice thickness and gap of DWI were identical to those of routine T1WI and T2WI. Sequential sampling of the k-space was used with echo-time (TE) = 110–135 msec and bandwidth = 1250 Hz/pixel, and 128 lines of data were acquired in 0.3 seconds. No parallel imaging technique was applied. Other parameters included a field-of-view = 240 mm, matrix size = 128 × 128, and the acquisition of four signals. All images were obtained while the patients maintained normal and consistent breathing, and a fat-saturated pulse was used for the DWI to exclude severe chemical-shift artifacts. A contrast-enhanced dynamic study was performed and postcontrast T1WI were obtained in all cases, the details of which are not given here, as they are out of the scope of this work.

DWI were acquired with motion-probing gradient pulses applied along three (x-, y-, and z-axes) directions with three b factors of 0, 500, and 1000 seconds/mm^2. ADC maps were automatically generated on the operating console using all seven images (b = 0 and two b-values in each direction), and the ADC values were obtained by measuring the intensity of the map.

Pathological Map Preparation

One experienced pathologist created transverse sections of the specimens: the most apical and basic sides of the specimen were cut to a thickness of 6 mm, and the remaining portion (majority of the specimen) were cut to a thickness of 4 mm. Each section of each specimen was digitally photographed together with a ruler along the edge, which serve as a size reference, and the areas of the PC that had been microscopically determined were marked on the digital photographs by the pathologist (pathological map) using commercially available presentation software (Microsoft PowerPoint 2002; Microsoft Corporation, Redmond, WA, USA). All PC foci, including infiltrating foci that did not form apparent masses, were marked on the map and divided into the sextants according to their location, as follows: right and left apices (lower third), midglands (middle third), and bases (upper third). Lesions consisting of uniform histological grades were also documented as such on the photograph. This pathological map was used as the gold standard in this study.

Assessment

First, we subdivided the glands of all patients into sextants on the MR images. The presence of PC in each sextant was retrospectively evaluated and recorded by two radiologists in a consensus. Initially, T2WI alone (T2WI reading) were interpreted and then T2WI and the ADC map (T2WI/ADC map reading) were interpreted. The readers were informed that the patients had undergone surgery for PC, but no other clinical information, (e.g., PSA level or biopsy results) was provided to the readers. On either T2WI or the ADC map, areas with apparently lower signal intensity than that of the surrounding tissue were considered to represent PC, according to the previously reported descriptions (5–16,21–25). Regarding T2WI/ADC map reading, when the findings on either sequence were equivocal, those on the ADC map were considered to have priority, if image degradation is not prominent. Sensitivity and specificity were thus calculated based on the sextant evaluation and the results of the two interpretations were compared.

We then directly compared the MR images and the pathological map on a lesion basis, and we excluded

positive sextants in which the noncancerous areas had been interpreted as PC on the MR images (false-positive lesions in positive sextants); thus the true sensitivity was calculated. As for a lesion whose location at least partially overlapped on the MR images and on the pathological map, the lesion was considered false-positive when the maximum transverse diameter measured at MRI was out of the range of 50% to 150% of the maximum transverse diameter measured on the pathological map (16). Lesions seen at MRI were only considered truly positive if the suspected foci were in the same relative portion of the prostate.

We also marked the approximate areas of PC on a pathological map, which had been detected on MR images (detected PC) using MR images as reference, and the areas of the whole PC and the detected PC were traced and measured using NIH software (NIH Image, version 1.63; National Institutes of Health, Bethesda, MD, USA). Volume was calculated by multiplying the measured areas by thickness (0.4 cm). False-positive lesions, including those in positive sextants as defined above, were excluded in this evaluation. Thus, % tumor volume (percentage of the tumor volume detected to the whole tumor volume; range = 0–100%) per patient was compared between the T2WI reading and T2WI/ADC map reading. The lesions were subclassified into peripheral zone (PZ) and transitional zone (TZ) lesions according to their location on the pathological map, and these two groups were compared in terms of % tumor volume per patient. Then, the % tumor volume per patient was also correlated to the GS of the patients.

Lesions with uniform histological grades that were larger than 1 cm in their short axes were selected on the pathological map and their ADC values were measured at the corresponding sites on the ADC map by one radiologist, even when there were no detectable abnormal areas on the ADC map. Correlation of ADC value and histological grades was thus evaluated. We also evaluated the detectability of these lesions in correlation with the their histological grades.

Finally, by comparing the MR images and pathological maps, we selected areas of PC larger than 1 cm in their short axes that had not been detected on ADC map (false-negative lesions). The possible reasons for these lesions not being detected on MR images were analyzed. We also selected areas of low signal intensity larger than 1 cm in their short axes on the ADC map that did not correspond to PC on the pathological map (false-positive lesions). The corresponding sites were marked on the pathological map, and pathological details of these areas were then reevaluated by the pathologist.

RESULTS

In one patient, microscopic evaluation of the resected gland revealed no PC, although preoperative biopsy had suggested the presence of PC in one of the sextants. A total of 222 sextants in 37 patients were evaluated, among which 147 sextants were positive and 75 were negative for the presence of PC. A total of 79 and 105 positive sextants, and 45 and 46 negative sextants were correctly diagnosed with T2WI reading and T2WI/ADC map reading, respectively. Among the 79 and 105 positive sextants that were classified as positive, 45 and 31 were excluded for the calculation of true sensitivity because they were regarded as noncancerous areas on the lesion-based evaluation. The sensitivity, true sensitivity, and specificity of T2WI reading were 53%, 23%, and 60%, whereas the sensitivity, true sensitivity, and specificity of the T2WI/ADC map reading were 71%, 50%, and 61%, respectively. There was a significant difference between the two interpretations in terms of the sensitivity and true sensitivity ($P < 0.01$, McNemar chi-squared test), but no difference in the specificity ($P = 0.97$).

The areas of PC on the pathological map ranged from 3 mm to 22 mm in their shortest dimension (mean = 7 mm). The calculated volumes of PC per patient ranged from 0 to 5.75 cm^3 (mean = 1.49 cm^3). There were 261 and 151 areas of the PC in PZ and TZ; the sum of tumor volume were 38.8 and 16.3 cm^3, respectively. The majority (33/37) of our patients had areas of PC in both PZ and TZ. The mean % tumor volume per patient detected by T2WI reading were 20% (range = 0–100%), 41% (range = 0–100%), and 7% (range = 0–91%), for total lesions, the PZ lesions, and TZ lesions, respectively. The mean % tumor volume per patient detected by T2WI/ADC map reading for total lesions, the PZ lesions, and TZ lesions, were 47% (range = 0–100%), 48% (range = 0–100%), and 44% (range = 0–100%), respectively. Overall (not per patient, but total sum) % tumor volume by T2WI reading were 30%, 55%, and 20%, for total lesions, the PZ lesions, and TZ lesions, respectively. Overall % tumor volume by T2WI/ADC map for total lesions, the PZ lesions, and TZ lesions, reading were 55%, 57%, and 52%, respectively. Addition of the ADC map to T2WI interpretation revealed a significant increase in % tumor volume in total lesions ($P = 0.0002$, Wilcoxon signed rank test) and in TZ lesions ($P < 0.0001$), but not in PZ lesions ($P = 0.158$, not significant [NS]).

For the resected specimens in 35 patients (excluding one patient whose specimen revealed no evidence of PC and another who had received hormonal therapy), GS were assigned. There was a weak but significant correlation between % tumor volume by T2WI/ADC map reading and GS ($\rho = 0.40$, $P = 0.022$, Spearman's rank correlation test) (Fig. 1). Patients with higher GS tended to have higher % tumor volume, namely had more chance for PC to be detected by T2WI/ADC map reading. No significant correlation was observed between % tumor volume detected by T2WI reading alone and GS ($P = 0.41$, NS). Because it has been reported that the larger the tumor is, there is the better correlation between tumor volume measured on T2WI and histopathologic volume (14), we might need to exclude the effect of the volume of PC in evaluating the correlation between % tumor volume by T2WI/ADC map reading and GS. We therefore evaluated the partial correlation coefficient between either tumor volume or GS and % tumor volume detected (Table 1). The results showed that % tumor volume detected with T2WI/ADC map reading significantly correlated to GS, but not to tumor volume, and also that % tumor volume detected with T2WI reading correlated to the tumor volume, but not to GS.

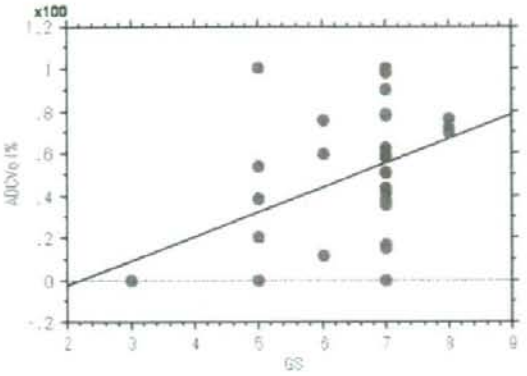

Figure 1. Correlation between % tumor volume detected by T2WI and ADC map interpretation and GS of the specimens. There was a weak but significant correlation ($\rho = 0.40$, $P = 0.022$, Spearman's rank correlation test). ADC Vol% = % tumor volume detected with T2WI and ADC map interpretation, GS = Gleason's scores.

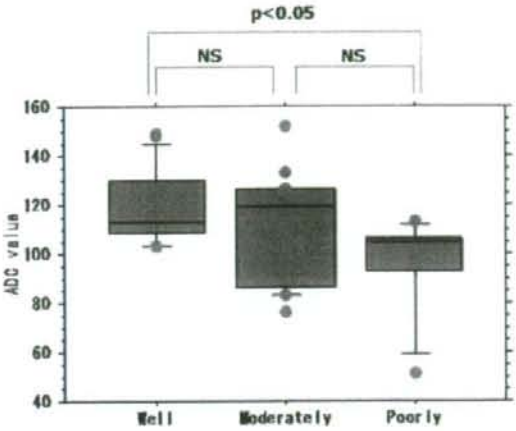

Figure 2. Correlation between ADC values and histological grades of PC. ADC values of well-, moderately-, and poorly-differentiated adenocarcinoma were 1.19 ± 0.15, 1.10 ± 0.24, and 0.93 ± 0.20 × 10^{-3} mm^2/second (mean ± SD), respectively. Difference was significant only between well- and poorly-differentiated carcinoma ($P = 0.019$, one-way factorial ANOVA with Scheffe's post-hoc test). There was a subtle, but significant correlation (Spearman's rank correlation test, $\rho = -0.144$, $P = 0.045$). A horizontal line in the middle of each box indicates a median of each group. [Color figure can be viewed in the online issue, which is available at www.interscience.wiley.com.]

Regarding the ADC value measurement, 53 lesions with uniform histological grades that were larger than 1 cm in their short axes were selected from 36 patients. There were 21, 26, and six lesions, in well-, moderately-, and poorly-differentiated adenocarcinomas, respectively. The mean size (short axis diameter) of these lesions was 1.14 cm (range: 1.0–1.9 cm), 1.23 cm (1.0–2.2 cm), and 1.03 cm (1.0–1.2), respectively, showing no significant difference ($P = 0.38$, one-way factorial analysis of variance [ANOVA]). The ADC values of well-, moderately-, and poorly-differentiated PC were 1.19 ± 0.15, 1.10 ± 0.24, and 0.93 ± 0.20 × 10^{-3} mm^2/second (mean ± standard deviation [SD]), respectively. Significant difference in ADC values was seen only between well- and poorly-differentiated PC ($P = 0.019$), and difference between well- and moderately-differentiated, or that between moderately- and poorly-differentiated PC was not significant ($P = 0.38$ and 0.13, one-way factorial ANOVA with Scheffe's post hoc test). There was a subtle but significant correlation between the histological grades and ADC values ($\rho = -0.18$, $P = 0.014$, Spearman's rank correlation) (Fig. 2). Of these 53 lesions, 13 (62%), 24 (92%), and six (100%) were detected on the ADC map, in well-, moderately-, and poorly-differentiated adenocarcinomas, respectively. The detectability of these lesions differed significantly among histological grades (Kruskal-Wallis test, $P < 0.01$) and a significant correlation was observed, whereby the less differentiated lesions were associated with higher detectability ($P < 0.01$, Cochran-Armitage test for trend).

Table 1
Partial Correlation Coefficient Based on Spearman's Rank Correlation Coefficient Between Either Tumor Volume or Gleason's Score and % Tumor Volume Detected by T2WI Reading Alone and T2WI/ADC Map Reading

	% Tumor volume detected	
	T2WI	T2WI/ADC map
Tumor volume		
Partial ρ	0.4439	0.045
P-value	0.0109	0.8065
Gleason's score		
Partial ρ	−0.0535	0.3507
P-value	0.7712	0.0491

T2WI = T2-weighted image reading, T2WI/ADC map = T2-weighted image and apparent diffusion coefficient map reading, ρ = correlation coefficient.

As for false-positive lesions, 54 foci were selected from 27 patients. The pathological details of these lesions included hyperplastic nodules in 22, normal structure in 14 (periejaculatory duct tissue in five, asymmetric central zone tissue in four, base of the seminal vesicle in three, asymmetric anterior fibromuscular stroma in one, and vermontanum in one), intraacinar hemorrhage in 10, and chronic prostatitis in eight. As for false-negative lesions, 15 foci in 15 patients were selected. Possible causes for these false-negatives were well-differentiated infiltrative lesions with preserved gland formation in six lesions, susceptibility artifact from rectal or intestinal gas in four lesions, and susceptibility artifact from metallic prosthesis at the hip joint in one lesion. Causes for the remaining four lesions remained unknown. Representative cases are shown in Figs. 3, 4, and 5.

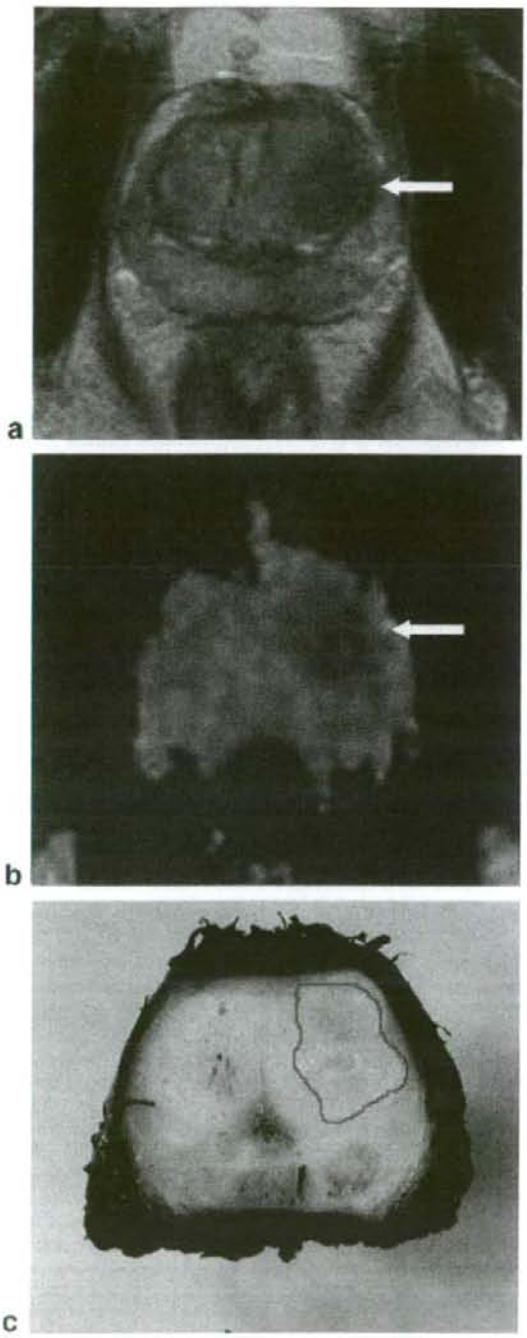

Figure 3. A 69-year-old man with a preoperative PSA level of 12.5 ng/mL. There was a moderately differentiated adenocarcinoma at the left TZ (GS: 3 + 5 = 8) confined within the gland. Both T2WI **(a)** and ADC map **(b)** clearly demonstrated carcinoma as low signal intensity areas (arrows). An encircled area represents the carcinoma on the pathological map **(c)**. [Color figure can be viewed in the online issue, which is available at www.interscience.wiley.com.]

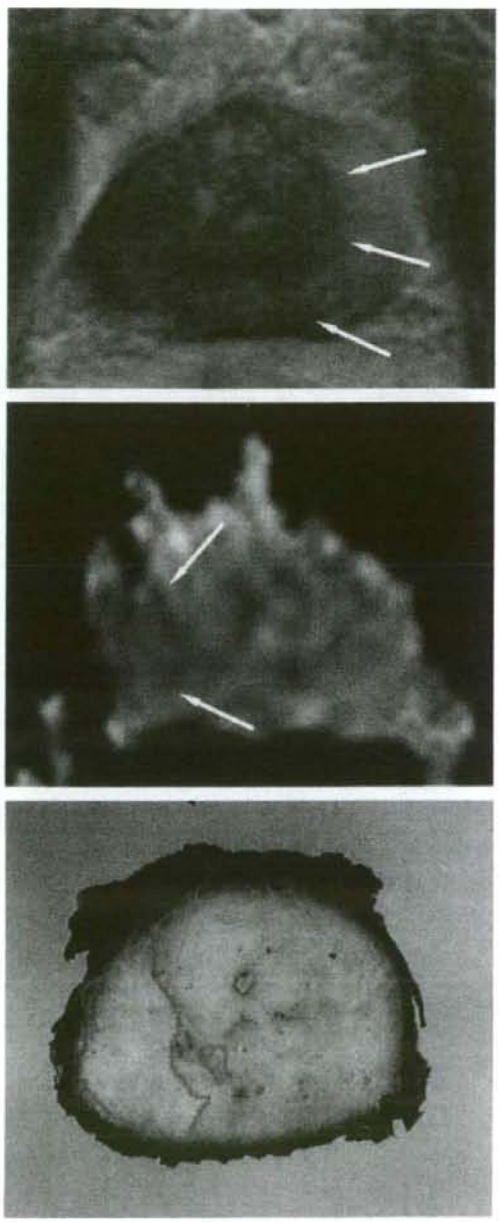

Figure 4. A 63-year-old male with an initial PSA level of 16 ng/mL. The patient received hormonal therapy using chrormadinone acetate and leuprorelin acetate for three months and the PSA level decreased to 0.8 ng/mL just before surgery. There was a moderately- to poorly-differentiated adenocarcinoma at the right PZ, confined within the gland. GS was not evaluated because of cellular degeneration. On T2WI **(a)**, approximately two-thirds of the gland on the right exhibited low signal intensity (arrows). On ADC map **(b)**, an area of low signal was localized at the right PZ (arrows), which corresponded well to the area of carcinoma shown on the pathological map **(c)** (encircled areas). [Color figure can be viewed in the online issue, which is available at www.interscience.wiley.com.]

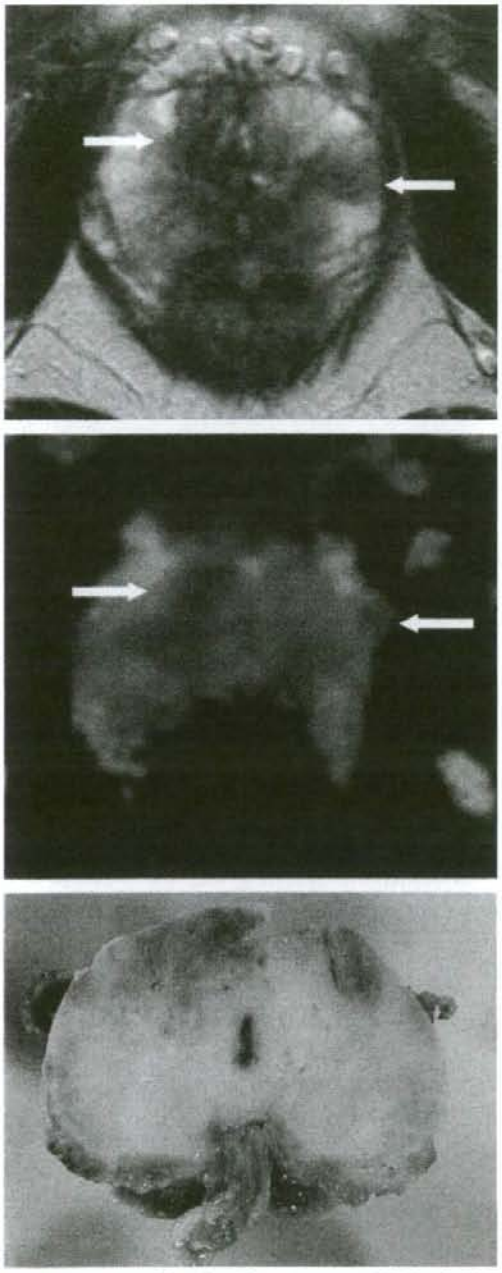

Figure 5. A 59-year-old male with a preoperative PSA level of 0.7 ng/mL and positive biopsy results. There was a small focus (3 mm in diameter) of well-differentiated adenocarcinoma at the apex of the gland (not shown), with a GS of 3 + 2 = 5. The major portion of the gland was free of carcinoma cells. There were several areas of low signal intensity, both on T2WI (**a**) and ADC map (**b**) (arrows); however, there was no carcinoma at the corresponding sites on the pathological map (**c**). Hyperplastic glandular and interstitial cells were noted at theses sites upon reevaluation of the specimen. [Color figure can be viewed in the online issue, which is available at www.interscience.wiley.com.]

DISCUSSION

Previous investigators have reported significant difference in ADC values between PC and normal prostatic tissue, using biopsy-proven histopathology as a reference (21–25). To date, there have been few reports regarding PC detection with DWI or ADC mapping in patients who had undergone prostatectomy. We therefore attempted in the present study to clarify the clinical usefulness and significance of DWI or ADC mapping using a stepwise histopathology as a gold standard.

According to our results, sextant-based sensitivity and true sensitivity improved significantly, i.e., up to 71% and 50%, respectively, when the ADC map was interpreted along with T2WI, although the specificity remained unchanged at around 60%. In terms of the volume of PC, T2WI/ADC map reading detected approximately one-half of the tumor in the gland. Previously reported sensitivity and/or detection rate of PC on MRI (i.e., T2WI with or without spectroscopy), has been in a range between 20% to 80% (6–16). Recently, Hom et al (16) reported a detection rate of around 20% using endorectal coil MR images and MR spectroscopy for cases of PC in PZ, and using meticulous histopathologic evaluation methods and strict criteria. Our data also revealed a rather low sensitivity or detection rate, at least in part because we also used the pathological map as a strict gold standard, including all small foci of PC. Another explanation for this low sensitivity may have been the criteria we used to detect PC in our study. Namely, we considered "areas with low signal intensity relative to the surrounding tissue" as PC in both PZ and TZ; however, Li et al (27) recently applied more meticulous criteria to diagnose TZ lesions and achieved better results. Although the application of different criteria might have improved the sensitivity, our present data suggest that a T2WI/ADC map reading cannot be used as a reasonable guide yet in localization of PC in the context of local therapies such as IMRT or HIFU. Practical use of ADC maps may therefore be limited at present, for example, to a guide for rebiopsy in patients with high PSA levels but with negative biopsy results.

To improve sensitivity of the T2WI/ADC map reading, it will be necessary to detect well-differentiated PC with glandular formation, which was the most common cause of false negativity in our series. In our evaluation of the lesions larger than 1 cm in the shortest dimension, the ADC values of well-differentiated PC were significantly higher than moderately- or poorly-differentiated PC, and nearly one-half of these lesions were visually missed on the T2WI/ADC map interpretation. The pathological architecture of these lesions, namely, preserved glandular formation with a significant volume of fluid-filled luminal space, which is similar to that of normal prostatic glandular tissue, supports the relatively high ADC values of these lesions; these features rendered it difficult to detect such lesions on the ADC map. Improving the signal-to-noise ratio (SNR) by using 3T hardware or a coil with more channels may help detect these lesions. Concurrent usage of a parallel imaging technique (24,28,29) may also help reduce the susceptibility artifacts, the second most common cause of false negativity.

To improve specificity, it will be necessary to differentiate between hyperplastic nodules and PC; the lack of such differentiation was the most common cause of false positivity in our results. Again, improving the SNR by either the use of 3T hardware or new coils may help differentiate these two entities. The second most common reason for false positivity was normal prostatic tissue, including periejaculatory duct tissue, central zone tissue, tissue at the base of the seminal vesicle, and so on. The ADC values of these structures were $0.97 \pm 0.18 \times 10^{-3}$ mm^2/second (not shown in the results), which were within the range of ADC values of PC. Precise anatomic evaluation may obviate this misdiagnosis; however, it would remain difficult to discriminate these structures from focal involvement of PC on an ADC map. Combination with MR spectroscopy or dynamic MR study may be of some help in resolving this problem.

The promising aspects of our findings are as follows. First, the T2WI/ADC map reading significantly increased the detection of PC located in TZ. In terms of the % tumor volume, the detection rate of T2WI/ADC map reading was approximately 50% regardless of the location of PC, whereas that of T2WI reading alone was significantly worse in the case of lesions in TZ than in those in PZ. Because PC in TZ has remained a diagnostic problem either for transrectal ultrasound (US) or conventional MR, use of DWI and ADC maps could be of aid in the detection of lesions in TZ in particular. Although Li et al (27) recently reported improved detection of PC in TZ using the combined criteria of T2WI and postcontrast T1WI, adding information of ADC map might further improve the detection of PC in TZ.

A second promising point suggested by our results was that the higher the histological grade of PC, the lower the ADC values of PC, which increases the chances of PC being detected on an ADC map. This finding may also be related to the positive correlation between % tumor volume detected by T2WI/ADC map reading and GS (Table 1). Such information may be clinically important because it may suggest that the biologically aggressive components or subsets of PC are more likely to be detected by T2WI/ADC map reading than would less aggressive components. As the histological grade or GS increases, there have been shown to be more chances of cellular architectures exhibiting little gland formation, such as medullary or solid patterns (30,31); these features may explain the low ADC values in these lesions. Although the ADC values obtained in our study were comparable to the previously reported values (21–25), this is the first study to reveal the relationship between histological grade or GS and ADC values in cases of PC.

A third promising issue suggested by the results from but a single patient was that the areas of PC was relatively clearly depicted on ADC map within areas of diffusely decreased signal intensity on T2WI; this was a patient who had received preoperative hormonal therapy (androgen deprivation) (Fig. 4). It was already well known that posthormonotherapy prostatic tissue becomes atrophic and diffusely hypointense, which impairs pertinent MR detection of PC (32,33). The ADC map might be of help in evaluating patients still undergoing or following hormonal therapy.

There are several limitations to the present study. First, this study was retrospective in nature, and all patients in this series had undergone biopsy prior to MR examination. Although the period between biopsy and MR examination in our study was more than one month, which is reportedly sufficient to avoid biopsy effects on MR images (34,35), the histopathological evaluation revealed intraacinar hemorrhage, which was the third most common cause of false positivity. Another technical aspect related to the retrospective nature of the study was the subtle differences between MR images and pathological section in terms of the slice interval and slice direction; such differences might have exerted an influence on the precise correlation between the depicted abnormality and the lesions observed on the pathological map. Prospective studies are needed that are designed in such a manner that MR examination is performed prior to biopsy and in which the MR and pathological sections are identical. In addition, due to the limitation associated with the hardware, TE of EPI used for the DWI was rather long (110–135 msec) in our study, as compared to that of previous reports (96–120 msec) (21–25). This long TE may have led to the low SNR of the images, particularly in cases involving tissues with short T2 characteristics, which in turn possibly led to the incorrect calculation of ADC values. Use of a parallel imaging technique might have improved this situation, allowing for a shorter TE (24,28,29), although this technique was not available at the time we started this study. Third, because of the significant image distortion of the ADC map, we did not perform any volume measurement on MR images, although in this study, such measurements were carried out on the pathological map by encircling the approximate area of PC by visual inspection using MR images as a reference. Again, a parallel imaging technique would have been useful to reduce the image distortion secondary to the susceptibility effect from intestinal gas or metallic prosthesis (24,28,29), which would in turn have enabled us to measure the areas of interest on the ADC map.

In conclusion, the ADC map derived from DWI of MRI performed with a phased array coil without parallel imaging technique significantly improved PC detection and localization when interpreted together with T2WI, although the performance of this method might not yet be sufficient for it to serve as a guide for local therapies. This novel approach to the diagnosis of PC is expected to be particularly useful for the detection of PC lesions located in TZ, as well as detection of lesions with relatively little differentiation, and lesions with a relatively high GS.

ACKNOWLEDGMENT

We thank Professor Masasumi Tsuneyoshi, Chair of the Department of Anatomic Pathology, Graduate School of Medical Sciences, Kyushu University, for providing us pathologic specimens for this study.

REFERENCES

1. American Cancer Society. Cancer Facts and Figures 2004. Atlanta, GA: American Cancer Society; 2004. 60 p. Available at: http://www.cancer.org/downloads/STT/CAFF_finalPWSecured.pdf. Last accessed: September 20, 2007.
2. Carroll PR, Presti JC Jr, Small E, Roach M III. Focal therapy for prostate cancer 1996: maximizing outcome. Urology 1997; 49(Suppl 3A):84–94.
3. Meerleer GD, Villeirs G, Bral S, et al. The magnetic resonance detected intraprostatic lesions in prostate cancer: planning and delivery of intensity-modulated radiotherapy. Radiother Oncol 2005;75:325–333.
4. Blana A, Walter B, Rogenhoer S, Wieland W. High-intensity focused ultrasound for the treatment of localized prostate cancer: 5-year experience. Urology 2004;63:297–300.
5. Rajesh A, Coakley FV. MR imaging and MR spectroscopic imaging of prostate cancer. Magn Reson Imaging Clin N Am 2004;12:557–579.
6. Engelbrecht MR, Huisman HJ, Laheij RJ, et al. Discrimination of prostate cancer from normal peripheral zone and central gland tissue by using dynamic contrast-enhanced MR imaging. Radiology 2003;229:248–254.
7. Hasumi M, Suzuki K, Taketomi A, et al. The combination of multivoxel MR spectroscopy with MR imaging improve the diagnostic accuracy for localization of prostate cancer. Anticancer Res 2003; 23:4223–4227.
8. Ikonen S, Kivisaari L, Tervahartiala P, Vehmas T, Taari K, Rannikko S. Prostatic MR imaging. Accuracy in differentiating cancer from other prostatic disorders. Acta Radiol 2001;42:348–354.
9. Dhingsa R, Qayyum A, Coakley FV, et al. Prostate cancer localization with endorectal MR imaging and MR spectroscopic imaging: effect of clinical data on reader accuracy. Radiology 2004;230:215–220.
10. Kurhanewicz J, Swanson MG, Nelson SJ, Vigneron DB. Combined magnetic resonance imaging and spectroscopic imaging approach to molecular imaging of prostate cancer. J Magn Reson Imaging 2002;16:451–463.
11. Kumar R, Kumar M, Jagannathan NR, Gupta NP, Hemal AK. Proton magnetic resonance spectroscopy with a body coil in the diagnosis of carcinoma prostate. Urol Res 2004;32:36–40.
12. Kiessling F, Huber PE, Grobholz R, et al. Dynamic magnetic resonance tomography and proton magnetic resonance spectroscopy of prostate cancers in rats treated by radiotherapy. Invest Radiol 2004;39:34–44.
13. Kaji Y, Wada A, Imaoka I, et al. Proton two-dimensional chemical shift imaging for evaluation of prostate cancer: external surface coil vs. endorectal surface coil. J Magn Reson Imaging 2002;16:697–706.
14. Coakley FV, Kurhanewicz J, Lu Y, et al. Prostate cancer tumor volume: measurement with endorectal MR and MR spectroscopic imaging. Radiology 2002;223:91–97.
15. Purohit RS, Shinohara K, Meng MV, Carroll PR. Imaging clinically localized prostate cancer. Urol Clin North Am 2003;30:279–293.
16. Hom JF, Coakley FV, Simko JP, et al. Prostate cancer: endorectal MR imaging and MR spectroscopic imaging—distinction of true-positive from chance-detected lesions. Radiology 2006;238:192–199.
17. Ichikawa T, Haradome H, Hachiya J, Nitatori T, Araki T. Diffusion-weighted MR imaging with a single-shot echoplanar sequence: detection and characterization of focal hepatic lesions. AJR Am J Roentgenol 1998;170:397–402.
18. Castillo M, Smith JK, Kwock L, Wilber K. Apparent diffusion coefficients in the evaluation of high-grade cerebral gliomas. AJNR Am J Neuroradiol 2001;22:60–64.
19. Nakayama T, Yoshimitsu K, Irie H, et al. Usefulness of the calculated apparent diffusion coefficient value in the differential diagnosis of retroperitoneal masses. J Magn Reson Imaging 2004;20:735–742.
20. Nakayama T, Yoshimitsu K, Irie H, et al. Diffusion-weighted echo-planar MR imaging and ADC mapping in the differential diagnosis of ovarian cystic masses: usefulness of detecting keratinoid substances in mature cystic teratomas. J Magn Reson Imaging 2005; 22:271–278.
21. Gibbs P, Tozer DJ, Liney GP, Turnbull LW. Comparison of quantitative T2 mapping and diffusion-weighted imaging in the normal and pathologic prostate. Magn Reson Med 2001;46:1054–1058.
22. Issa B. In vivo measurement of the apparent diffusion coefficient in normal and malignant prostatic tissues using echo-planar imaging. J Magn Reson Imaging 2002;16:196–200.
23. Hosseinzadeh K, Schwarz SD. Endorectal diffusion-weighted imaging in prostate cancer to differentiate malignant and benign peripheral zone tissue. J Magn Reson Imaging 2004;20:654–661.
24. Sato C, Naganawa S, Nakamura T, et al. Differentiation of noncancerous tissue and cancer lesions by apparent diffusion coefficient values in transition and peripheral zones of the prostate. J Magn Reson Imaging 2005;21:258–262.
25. Shimousa R, Fujimoto H, Akamata H, et al. Diffusion-weighted imaging of prostate cancer. J Comput Assist Tomogr 2005;29:149–153.
26. World Medical Association. Declaration of Helsinki: ethical principles for medical research involving human subjects. Ferney-Voltaire, France: World Medical Association; 2004. 5p. Available at: http://www.wma.net/e/policy/b3.htm. Last accessed: September 20, 2007.
27. Li H, Sugimura K, Kaji Y, et al. Conventional MR capabilities in the diagnosis of prostate cancer in the transition zone. AJR Am J Roentgenol 2006;186:729–742.
28. Sodickson DK, McKenzie CA. A generalized approach to parallel magnetic resonance imaging. Med Phys 2001;28:1629–1643.
29. Jaermann T, Crelier G, Pruessmann KP, et al. SENSE-DTI at 3 T. Magn Reson Med 2004;51:230–236.
30. Gleason DF, Vacu RG. Histologic grading and clinical staging of prostatic carcinoma. In: Tannenbaum M, editor. Urologic pathology: the prostate. Philadelphia: Lea and Febiger; 1997. p 171–197.
31. Epstein JI. Urinary tract and male genital system. The prostate and seminal vesicle. In: Sternberg SS, editor. Diagnostic surgical pathology. New York: Raven Press; 1989. p 1393–1432.
32. Chen M, Hricak H, Kalbhen CL, et al. Hormonal ablation of prostatic cancer: effects on prostate morphology, tumor detection, and staging by endorectal coil MR imaging. AJR Am J Roentgenol 1996; 166:1157–1163.
33. Padhani AR, MacVicar AD, Gapinsli CJ, et al. Effects of androgen deprivation on prostatic morphology and vascular permeability evaluated with MR imaging. Radiology 2001;218:365–374.
34. White S, Hricak H, Forstner R, et al. Prostate cancer: effect of post-biopsy hemorrhage on interpretation of MR images. Radiology 1995;195:385–390.
35. Ikonen S, Kivisaari L, Vehmas T, et al. Optimal timing of post-biopsy MR imaging of the prostate. Acta Radiol 2001;42:70–73.